IIETA International Information and Engineering Technology Association
Advancing the World of Information and Engineering

Mathematical Modelling of Engineering Problems
Vol. 12, No. 12, December, 2025, pp. 4345-4353
Journal homepage: http://iieta.org/journals/mmep

The Spread of African Swine Fever (ASF) in East Nusa Tenggara, Indonesia, Analyzed Using a Mathematical Modeling Approach

Ariyanto[1*], Maria Lobo[1], Farly Oktriany Haning[1], Keristina Br Ginting[1], Jusrry Rosalina Pahnael[1], Elisabet Tangkonda[2]

[1] Mathematics Study Program, Nusa Cendana University, East Nusa Tenggara 85001, Indonesia
[2] Department of Microbiology, Faculty of Medicine and Veterinary Medicine, Nusa Cendana University, East Nusa Tenggara 85001, Indonesia

Corresponding Author Email: aryanto@staf.undana.ac.id

https://doi.org/10.18280/mmep.121223

Received: 8 September 2025
Revised: 5 November 2025
Accepted: 13 November 2025
Available online: 31 December 2025

Keywords:
African swine fever, model mathematical, basic reproduction number, biosecurity strategy, optimal control, vector ticks

ABSTRACT

African swine fever (ASF) is a highly contagious viral disease that results in very high mortality rates among pigs and causes significant economic losses worldwide. In Indonesia, ASF has spread to 32 provinces since the first outbreak in 2019, with East Nusa Tenggara being one of the most severely affected areas. This study developed a nonlinear differential equation model to analyze the dynamics of ASF transmission and evaluate the combined effectiveness of biosecurity measures and vector control strategies in controlling the disease's spread. The model calculates the basic reproductive number both without and with vectors. An integrated approach that combines biosecurity measures and optimal vector control can significantly reduce the risk of infection, depending on the effectiveness of biosecurity (p) and the effectiveness of tick vector control (q). These findings suggest that the synergistic approach of combining biosecurity and optimal vector control is highly effective in reducing the spread of ASF in East Nusa Tenggara. This provides a scientific foundation for developing adaptive disease control policies in Indonesia.

1. INTRODUCTION

ASF is a highly virulent viral disease affecting both domestic and wild pigs, causing significant socioeconomic losses to the pig industry [1]. Globally, ASF is estimated to cause annual economic losses exceeding USD 2 billion [2]. In Indonesia, ASF was first detected in North Sumatra in 2019 and subsequently spread to 32 provinces [3]. East Nusa Tenggara Province experienced ASF outbreaks in 2020 and 2021, resulting in extremely high pig mortality, with cumulative losses reaching several hundred thousand animals [4]. ASF cases in the East Nusa Tenggara region continue to exhibit a high incidence rate up to 2025, and this situation generates substantial economic losses for smallholder farmers whose livelihoods rely heavily on pig production. To date, no vaccine or commercial antiviral drug has been proven effective against ASF [5]. Implementing strict biosecurity remains the most effective prevention strategy [6]. In East Nusa Tenggara, local farmers implement traditional and adaptive practices, such as installing mosquito nets around pens, to minimize contact with potential vectors [7]. These local initiatives highlight the vital importance of community-based biosecurity in areas with limited veterinary infrastructure. Mathematical modeling serves as a key tool for understanding disease transmission dynamics and developing effective control strategies [2].

Various mathematical models have been developed to study the dynamics of ASF transmission. Chuchard et al. [7] proposed a human-mediated transmission pathway, while Ayihou et al. [8]. Developed an eight-compartment model that yielded a fundamental reproduction number value, which indicates a high level of transmission based on analysis of Benin data. Kouidere et al. [9] further proposed an ASF transmission model that integrates vector dynamics and optimal control theory to formulate effective management intervention strategies.

The mathematical models currently developed primarily focus on either the African or European context, which means they do not accurately reflect the ecological, cultural, and agricultural conditions in Indonesia, particularly in East Nusa Tenggara. Recent research on ASF in this region can be found in the articles by Bulu et al. [10] and Pandarangga et al. [11]. Small-scale pig farming in East Nusa Tenggara is closely associated with varying levels of biosecurity practices, as well as the high mobility of pigs and people. Existing models often overlook these critical factors and seldom incorporate local biosecurity knowledge with vector control strategies. As a result, a research gap remains in understanding ASF transmission within the unique context of Indonesian veterinary environmental health.

The novelty of this study lies in the development of a nonlinear differential equation system model that explicitly represents the dynamics of ASF. This model integrates biosecurity and vector control interventions to evaluate their

effectiveness. The findings are expected to provide a scientific foundation for formulating ASF control policies that are adaptable to the sociocultural conditions in East Nusa Tenggara.

2. MATERIALS AND METHODS

2.1 Mathematical model formulation

In this study, we developed a model that consists of five compartments termed as susceptible pigs (S_p), exposed pigs (E_p), infected pigs (I_p), susceptible ticks (S_v), and infected ticks (I_v). This compartmental structure is an extension of the model proposed by Kouidere et al. [2]. The model examined in this study can be formulated as follows.

$$\begin{aligned}
\frac{dS_p}{dt} &= \Lambda_p - \beta_1 \frac{S_p I_p}{N_p} - \beta_2 \frac{S_p I_v}{N_p} - \mu_p S_p \\
\frac{dE_p}{dt} &= \beta_1 \frac{S_p I_p}{N_p} + \beta_2 \frac{S_p I_v}{N_p} - \gamma E_p - \mu_p E_p \\
\frac{dI_p}{dt} &= \gamma E_p - \mu_p I_p \\
\frac{dS_v}{dt} &= \Lambda_v - \beta_3 \frac{S_v I_p}{N_v} - \mu_v S_v \\
\frac{dI_v}{dt} &= \beta_3 \frac{S_v I_p}{N_v} - \mu_v I_v
\end{aligned} \tag{1}$$

where,

- Λ_p: The recruitment rate of susceptible pigs.
- Λ_v: The recruitment rate of susceptible ticks.
- β_1: The transmission rate of the virus among pigs through direct contact with infected pigs.
- β_2: The virus transmission rate to pigs through direct contact with infected ticks.
- β_3: The infection rate of ticks through direct contact with infected pigs.
- γ: The transition rate from E_p to I_p.
- μ_p: The natural mortality rate of pigs.
- μ_v: The natural mortality rate of ticks.

Let and denote the total pig and tick population, respectively, assumed to be constant. Based on Eq. (1), the following result is obtained:

$$\Lambda_p = \mu_p N_p \, and \, \Lambda_v = \mu_v N_v \tag{2}$$

From Eqs. (1) and (2), we can obtain the disease-free equilibrium, which represents a system state where there is no infection.

$$E_0 = \left(N_p, 0, 0, N_v, 0\right) \tag{3}$$

2.2 Basic reproduction number

The Next Generation Matrix (NGM) method was used to derive the basic reproduction number, as formulated in references by Bani-Yaghoub et al. [12] and Ndii et al. [13], where the transmission matrix ($\mathcal{F}$) and transition matrix ($\mathcal{V}$) are defined.

$$\mathcal{F} = \begin{pmatrix} \beta_1 \frac{S_p I_p}{N_p} + \beta_2 \frac{S_p I_v}{N_p} \\ 0 \\ 0 \end{pmatrix} \tag{4}$$

$$\mathcal{V} = \begin{pmatrix} -\gamma E_p - \mu_p E_p \\ \gamma E_p - \mu_p I_p \\ \beta_3 \frac{s_v I_p}{N_v} - \mu_v I_v \end{pmatrix} \tag{5}$$

From Eqs. (4) and (5), the following result is obtained:

$$F = \begin{pmatrix} 0 & \beta_1 & \beta_2 \\ 0 & 0 & 0 \\ 0 & 0 & 0 \end{pmatrix} \tag{6}$$

$$V^{-1} = \begin{pmatrix} -\frac{1}{\gamma + \mu_p} & 0 & 0 \\ -\frac{\gamma}{\mu_p \left(\gamma + \mu_p\right)} & -\frac{1}{\mu_p} & 0 \\ -\frac{\gamma \beta_3}{\mu_p \mu_v \left(\gamma + \mu_p\right)} & -\frac{\beta_3}{\mu_p \mu_v} & -\frac{1}{\mu_v} \end{pmatrix} \tag{7}$$

The next-generation matrix is obtained from $-TV^{-1}$, as follows:

$$K = \begin{pmatrix} \frac{\gamma \beta_1}{\mu_p \left(\gamma + \mu_p\right)} + \frac{\gamma \beta_2 \beta_3}{\mu_p \mu_v \left(\gamma + \mu_p\right)} & \frac{\beta_1}{\mu_p} + \frac{\beta_2 \beta_3}{\mu_p \mu_v} & \frac{\beta_2}{\mu_v} \\ 0 & 0 & 0 \\ 0 & 0 & 0 \end{pmatrix} \tag{8}$$

According to Eq. (8), the basic reproduction number (R_0) is termed as the spectral radius of the NGM. Hence, the value of R_0 is given as follows:

$$\mathcal{R}_0 = \frac{\gamma \beta_1}{\mu_p \left(\gamma + \mu_p\right)} + \frac{\gamma \beta_2 \beta_3}{\mu_p \mu_v \left(\gamma + \mu_p\right)} \tag{9}$$

Furthermore, the basic reproduction number, which explains the interaction between susceptible and infected pigs without the involvement of vector ticks, is given as follows:

$$\mathcal{R}_{01} = \frac{\gamma \beta_1}{\mu_p \left(\gamma + \mu_p\right)} \tag{10}$$

If $\mathcal{R}_0 < 1$, the disease will be eliminated from the population, whereas if $\mathcal{R}_0 > 1$, it is likely to spread more rapidly [14].

2.3 Model analysis

In this section, we will discuss the key properties of system (1), including the invariant region, positivity of solutions, and stability analysis of equilibrium points.

Invariant region and positivity of solution

Attention is restricted to the feasible region $\Omega = \Omega_p \times \Omega_v \subset R_+^3 \times R_+^2$, with:

$$\Omega_p = \left\{ \left(S_p, E_p, I_p\right) \in R_+^3 : N_p \leq \frac{\Lambda_p}{\mu_p} \right\} \tag{11}$$

$$\Omega_v = \left\{ \left(S_v, I_v\right) \in R_+^2 : N_v \leq \frac{\Lambda_v}{\mu_v} \right\} \tag{12}$$

Here are the results for the feasible region. The following three theorems are derived from the reference by Dayap and Rabajante [15] and Sasongko et al. [16].

Theorem 2.3.1 The region $\Omega = \Omega_p \times \Omega_v \subset R_+^3 \times R_+^2$ constitutes a positive invariant set for system (1) under non-negative initial conditions.

Proof: The summation of the ticks and pigs population in system (1) yields the following result:

$$\frac{dN_v}{dt} = \Lambda_v - \mu_v N_v \tag{13}$$

$$\frac{dN_p}{dt} = \Lambda_p - \mu_p N_p \tag{14}$$

Solving Eqs. (13) and (14) for N_v and N_p yields the bounded system $N_v \leq \frac{\Lambda_v}{\mu_v}$ and $N_p \leq \frac{\Lambda_p}{\mu_p}$.

Consequently, all feasible solutions of system (1) lie within the region.

Theorem 2.3.2 Let the system (1) have non-negative initial conditions. Then, its solution set is given by $\left(S_p(t), E_p(t), I_p(t), S_v(t), I_v(t)\right)$ and solution is non-negative for all $t > 0$.

Proof: To prove that system (1) has non-negative solutions for all $t > 0$, we first establish the positivity of $E_p(t)$, while the positivity of the remaining state variables follows by analogous arguments.

Assume the system is subject to non-negative initial conditions. From system (1), the following inequality holds:

$$\frac{dE_p}{dt} \geq -\left(\gamma + \mu_p\right) E_p \tag{15}$$

Eq. (15) takes the following form:

$$E_p(t) \geq E_p(0) e^{-(\gamma+\mu_p)t} \tag{16}$$

Since the initial condition $E_p(0)$ is non-negative and $e^{-(\gamma+\mu_p)t}$ is also non-negative, it follows that $E_p(t)$ remains non-negative for all $t \geq 0$.

Theorems 2.3.1 and 2.3.2 establish that system (1) well-posed and biologically meaningful.

Theorem 2.3.3 The disease-free equilibrium (DEF) E_0 of the system (1) is locally asymptotically stable when $\mathcal{R}_0 < 1$; otherwise, it becomes unstable.

Proof: To find the local stability of the DFE at E_0, the Jacobian matrix of system (1) will be derived as follows:

$$J\left(E_0\right) = \begin{pmatrix} -\mu_p & 0 & -\beta_1 & 0 & -\beta_2 \\ 0 & -\gamma-\mu_p & \beta_1 & 0 & \beta_2 \\ 0 & \gamma & -\mu_p & 0 & 0 \\ 0 & 0 & -\beta_3 & -\mu_v & 0 \\ 0 & 0 & \beta_3 & 0 & -\mu_v \end{pmatrix} \tag{17}$$

From the Jacobian matrix $J(E_0)$ above, the following characteristic polynomial is obtained:

$$p(\lambda) = \left(\mu_p + \lambda\right)(\mu_v + \lambda)\left(\lambda^3 + a_1\lambda^2 + a_2\lambda + a_3\right) = 0$$

with

$$\begin{aligned} a_1 &= 2\mu_p + \mu_v + \gamma \\ a_2 &= \mu_v\left(\gamma + \mu_p\right) + \mu_p\mu_p + \mu_p(\gamma + \mu_v)(1 - R_0) \\ &\quad + \frac{\gamma\beta_2\beta_3(\gamma + \mu_v)}{\mu_v\left(\gamma + \mu_p\right)} \\ a_3 &= \mu_p\mu_v\left(\gamma + \mu_p\right)(1 - R_0) \end{aligned}$$

The characteristic equation $p(\lambda)$ of $J(E_0)$ yields the eigenvalues $\lambda_1 = -\mu_p$, $\lambda_2 = -\mu_v$, and $\lambda^3 + a_1\lambda^2 + a_2\lambda + a_3 = 0$. By the Routh-Hurwitz, all roots are negative provide that $a_1 > 0$, $a_3 > 0$ and $a_1 a_2 > a_3$ whenever $R_0 < 1$. Hence, the equilibrium point E_0 is stable if $\mathcal{R}_0 < 1$. Conversely, if $\mathcal{R}_0 > 1$, the equilibrium point E_0 becomes unstable.

3. RESULTS

3.1 The constructed estimation of $\mathcal{R}_0$ according to the interaction between susceptible and infected pigs without vector ticks involved

First, we construct the estimation of $\mathcal{R}_{01}$ from Eq. (10). This estimation at E_0 is based on the assumption that the number of infected pigs, I_p, grows exponentially at the same rate over a short period of time [17].

$$E_p(t) = E_p(0)e^{rt} \tag{18}$$

$$I_p(t) = I_p(0)e^{rt} \tag{19}$$

with $E_p(0)$ and $I_p(0)$ denoting the initial numbers of exposed and infectious pigs, respectively, and let r represent the take-off rate of the early epidemic growth. Next, by substituting (18) and (19) into (1) and assuming $E_p \approx S_p$ and

$I_p \approx S_p$ at the early stage of the epidemic, we obtain:

$$\mathcal{R}_{01est} = \left(1+\frac{r}{\mu_p}\right)\left(1+\frac{r}{\gamma+\mu_p}\right) \tag{20}$$

with

$$\beta_1 = \frac{\left(r+\gamma+\mu_p\right)\left(r+\mu_p\right)}{\gamma} \tag{21}$$

The values of the model parameters and their corresponding sources are presented in Table 1.

The data of ASF cases in East Nusa Tenggara Province, Indonesia, are displayed in Figure 1.

Figure 1 displays the monthly incidence of ASF in East Nusa Tenggara, Indonesia, which reached its highest peak in January 2021. This will be used as the basis for estimating the $\mathcal{R}_0$ value.

Table 1. Parameter value and references

Parameter	Value	Source
μ_p	0.16667 month^{-1}	[18]
γ	2.73 month^{-1}	[19]
μ_v	0.017 month^{-1}	[20]

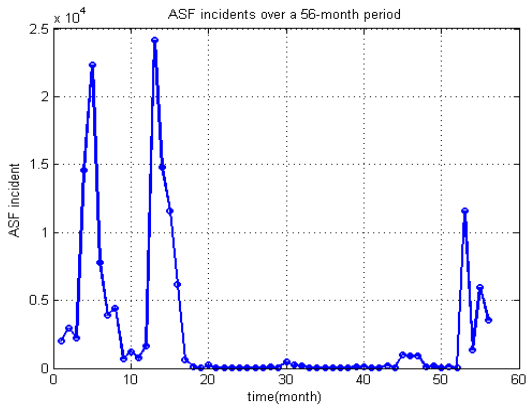

Figure 1. ASF cases incidence in East Nusa Tenggara from 2020 to 2025

Figure 1 presents the monthly ASF incidence in East Nusa Tenggara, Indonesia, with the highest peak observed in January 2021. This dataset forms the basis for estimating the early epidemic growth rate and the basic reproduction number $\mathcal{R}_0$.

Figure 2 displays the fitted model curve together with the observed ASF incidence. The close visual agreement between the model output and the reported data supports the reliability of the estimated take-off rate and the basic reproduction number $\mathcal{R}_0$. The analysis yields a take-off rate $r = 0.2$ (95% $CI: 0.1854 - 0.2566$) with a coefficient of determination $R^2 = 0.7763$, indicating a strong correspondence between the model and the observed data, as well as stable estimate with minimal uncertainty. Using the parameter values provided in Table 1, together with $r = 0.2$ and Eqs. (20) and (21), the basic reproduction number is estimated as $\mathcal{R}_{01} = 2.35$ for $\beta_1 = 0.4$. The transmission potential of ASF pigs is higher than through ticks, as the virus spreads more readily via direct contact with bodily fluids [20]. Given the limited field data on ASF-infected ticks, this study assumes that β_2 is 32% of β_1, and β_3 is 22% of β_2, yielding $\beta_2 = 0.128$, and $\beta_3 = 0.0282$. Thus, based on Eq. (9) and the parameter values in Table 1, including β_2 and β_3, the basic reproduction number involving transmission through infected ticks vectors is obtained $\mathcal{R}_0 = 3.5$. Several $\mathcal{R}_0$ values from different countries are presented for comparison with the $\mathcal{R}_0$ value in East Nusa Tenggara.

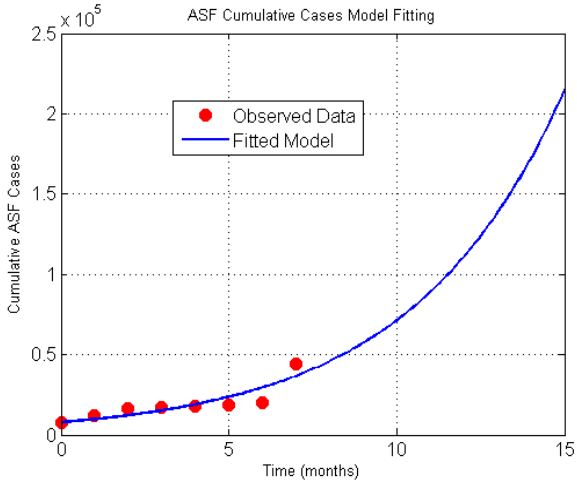

Figure 2. The fitting between observational data and fitted model

The reproduction number of ASF transmission in East Nusa Tenggara is relatively high compared to cases in other countries, as shown in Table 2.

Table 2. Values of $\mathcal{R}_0$ several countries

Country	$\mathcal{R}_0$ Value	Source
Benin	2.78	[8]
Uganda	3.24	[21]
Czech Republic	1.95	[22]
Belgium	1.65	[23]

3.2 A mathematical model with biosecurity measures and contact control between susceptible pigs and ASF-infected ticks

The model incorporating biosecurity measures and contact control between susceptible pigs and ASF-infected ticks is formulated as follows:

$$\begin{aligned}
\frac{dS_p}{dt} &= \Lambda_p - (1-p)\beta_1 \frac{S_p I_p}{N_p} - \beta_2 (1-q)\frac{S_p I_v}{N_p} - \mu_p S_p \\
\frac{dE_p}{dt} &= (1-p)\beta_1 \frac{S_p I_p}{N_p} + (1-q)\beta_2 \frac{S_p I_v}{N_p} - \gamma E_p - \mu_p E_p \\
\frac{dI_p}{dt} &= \gamma E_p - \mu_p I_p \\
\frac{dS_v}{dt} &= \Lambda_v - \beta_3 \frac{S_v I_p}{N_v} - \mu_v S_v \\
\frac{dI_v}{dt} &= \beta_3 \frac{S_v I_p}{N_v} - \mu_v
\end{aligned} \tag{22}$$

where, p denotes the effectiveness of biosecurity measures in reducing transmission between pigs, and q denotes the

effectiveness of controlling ASF-infected ticks. By applying the NGM method as in the previous concept, the basic reproduction number derived from Eq. (22) is obtained as follows:

$$\mathcal{R}_0 = \frac{(1-p)\gamma\beta_1}{\mu_p\left(\gamma+\mu_p\right)} + \frac{(1-q)\gamma\beta_2\beta_3}{\mu_p\mu_v\left(\gamma+\mu_p\right)} \tag{23}$$

3.3 Numerical simulation

We performed numerical simulation to evaluate the time to disease extinction within the system and to identify the conditions that facilitate the emergence of an endemic state in the population. The simulation results are presented in Figures 3 and 4.

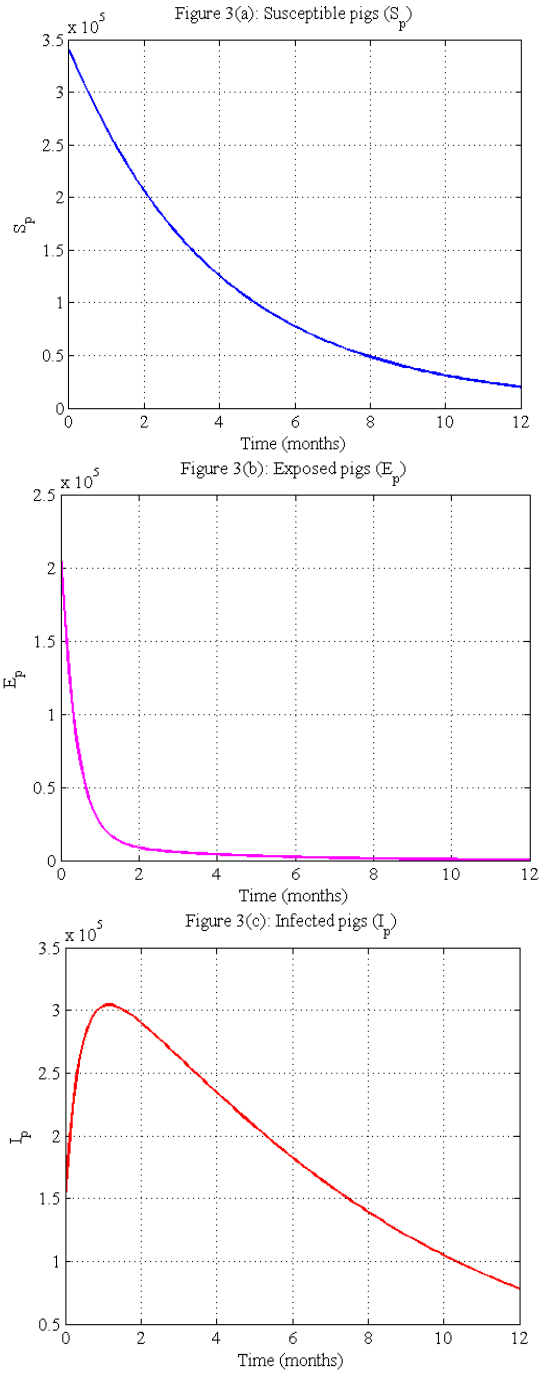

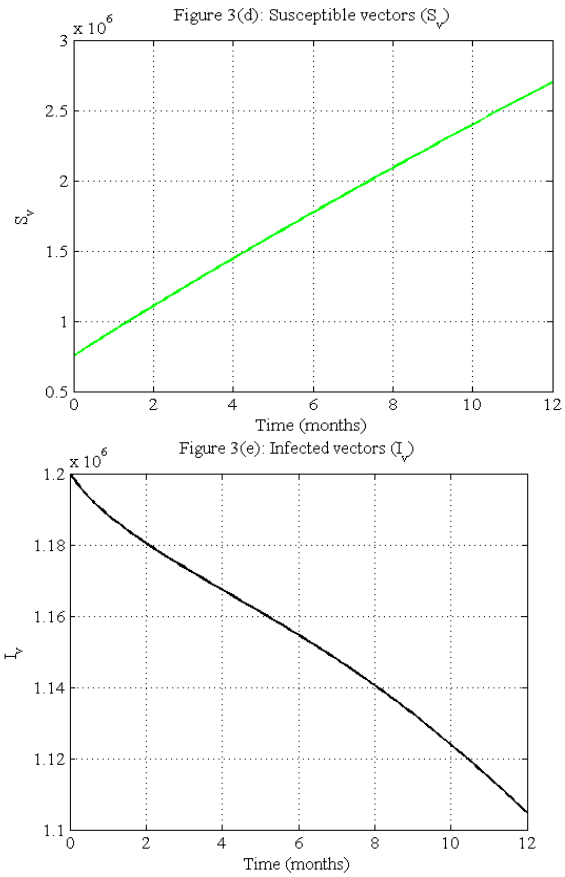

Figure 3. Numerical simulation of disease extinction in the population

Figure 3(a) shows a monotonic, near-exponential decline approximately 3.4×10^5 at the beginning of the observation period to about 0.2×10^5 by month 12, indicating a consistent depletion of the susceptible population throughout the study.

The E_P compartment exhibits a pronounced transient dynamic, marked by a sharp decline during the first 0–2 months from approximately 2.0×10^5 to nearly zero, after which it remains at a very low level for the remainder of the time horizon. This pattern indicates that the exposure phase is short-lived before the system stabilizes near zero.

Figure 3(c) illustrates a wave-like infection dynamic, in which I_P increases rapidly from approximately 1.6×10^5 to a peak of 3.0×10^5 arround month 1, followed by a gradual decline to about 0.8×10^5 by month 12. This pattern reflects an initial amplification phase of infection, followed by a subsequent dissipation phase as the system approaches a lower level of infectivity.

Figure 3(d) shows that the S_v compartment exhibits an approximately linear upward trend, increasing from about 0.8×10^6 to around 2.7×10^6 over the 12-month horizon. This pattern indicates a steady expansion of the susceptible vector population throughout the study period.

Figure 3(e) shows a gradual decline from approximately 1.2×10^6 to about 1.11×10^6 by month 12, with a slightly steeper gradient toward the end of the time horizon. This pattern reflects a slow but continuous dissipation of the infected vector population throughout the study period.

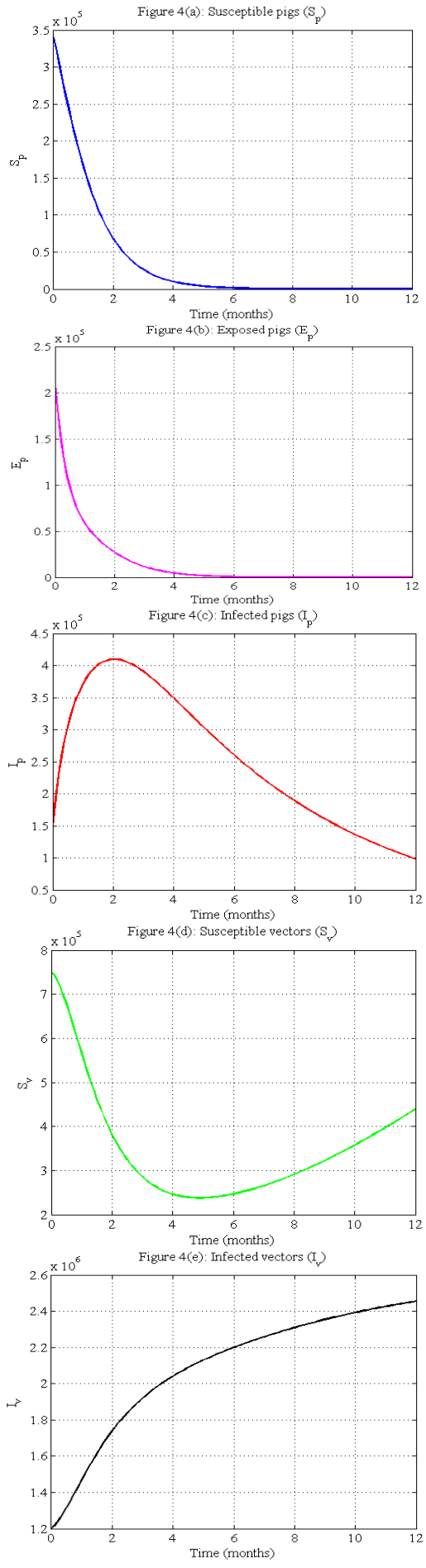

Figure 4. The numerical solution is examined under conditions in which the disease persists within the population

Figure 4(a) shows that the susceptible pig population S_p declines rapidly to near zero within approximately 5–6 months. This pattern suggests a high effective transmission pressure, leading to a rapid depletion of susceptibles through progression to infection-related compartments (or removal). Thereafter, the system approaches an endemic steady state with a very small susceptible pool.

Figure 4(b) illustrates the temporal evolution of the exposed pig population, E_p, over 12 months. The population experiences a sharp decline during the initial phase, with the most pronounced reduction occurring between months 2 and 3. By month 5–6, E_p approaches zero and remains negligible, indicating a rapid depletion of the exposed class and the system's convergence toward an almost disease-free state.

Figure 4(c) illustrates the unimodal temporal of I_p. The infected pig population increases rapidly during the initial phase, reaching a peak of approximately 4.1×10^5 in month 2, and subsequently declines gradually and near-monotonically to about 1.0×10^5 by month 12. This trajectory suggests a transient early outbreak followed by relaxation toward a quasi-endemic regime.

Figure 4(d) indicates that the susceptible vector population S_v declines sharply during the initial phase, decreasing from approximately 7.5×10^5 to a minimum of $(2.4 - 2.6) \times 10^5$ around months 4–5, before rising steadily to about 4.4×10^5 by month 12. This trajectory reflects an early depletion of susceptible vectors followed by progressive recovery toward a quasi-equilibrium state.

Figure 4(e) indicates that I_v increases monotonically, rising rapidly during the initial phase from approximately 1.2×10^6, and then shifting to a slower growth rate that approaches saturation, reaching $(2.4 - 2.5) \times 10^6$ by month 12. This trajectory suggests a sustained accumulation of infected vector as the system moves toward a quasi-endemic regime.

In this section, the effects of parameters p and q on the dynamics of E_p are examined via numerical simulations, by analyzing the temporal response of E_p across a range of (p, q) values and identifying the combinations that most effectively reduce exposure.

Figure 5 presents the simulation results for the reduction in the exposed compartment E_p as the parameters p and q increase. The percentage reduction in E_p is used as an indicator of the effectiveness of biosecurity (p) and contact control between susceptible pigs and ASF-infected ticks (q). Specifically, when p = 50% and q = 50%, E_p decreases by 17.48%. When p = 65% and q = 65%, the reduction in E_p increases to 22.73%, then to 25.18% for p = 72% and q = 72%, and reaches 29.72% for p = 85% and q = 85%. These findings indicate that strengthening biosecurity and contact control measures consistently reduces the proportion of pigs in the exposed compartment.

Next, the decline in the basic reproduction number $\mathcal{R}_0$ is analyzed in response to intervention strategies represented by variations in parameters p and q. This analysis examines how changes in p and q influence $\mathcal{R}_0$ to identify the most effective combination of interventions for reducing transmission potential.

Figure 6 presents the simulated reduction in the basic reproduction number $\mathcal{R}_0$ as the parameters p and q increase. Quantitatively, when p = 50% and q = 50%, $\mathcal{R}_0$ = 1.175; at p = 65% and q = 65%, $\mathcal{R}_0$ decreases to 1.2425; and for p = 72% and q = 72%, $\mathcal{R}_0$ is further reduced to 0.994. At a higher

level of intervention, namely p = 85% and q = 85%, $\mathcal{R}_0$ declines further to 0.5325. Overall, these results indicate that enhanced biosecurity and contact control are effective in reducing $\mathcal{R}_0$ to below one, thereby suggesting the potential for outbreak control from an epidemiological perspective.

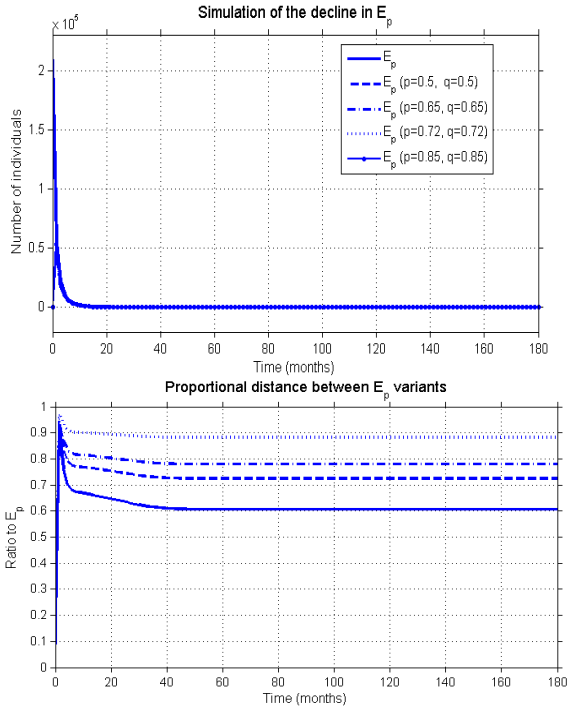

Figure 5. Simulation of changes in E_p resulting from variation in the parameters p and q

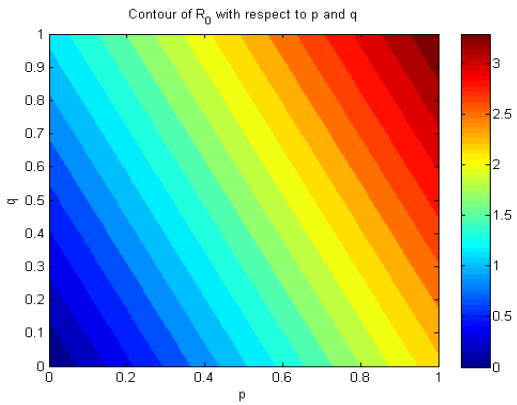

Figure 6. Simulation of changes in $\mathcal{R}_0$ in response to variation in parameters p and q

3.4 Sensitivity analysis

Local sensitivity analysis is applied when a small number of parameters are uncertain, with an approach based on the concept of partial derivatives [24-26]. The normalized sensitivity index formula used in this study is as follows:

$$C_p = \frac{\partial \mathcal{R}_0}{\partial p} \frac{p}{\mathcal{R}_0}$$

where, p denotes a parameter.

The normalized sensitivity indices of the parameters γ, β_1, and β_2 with respect to $\mathcal{R}_0$ are presented in Figure 7, respectively.

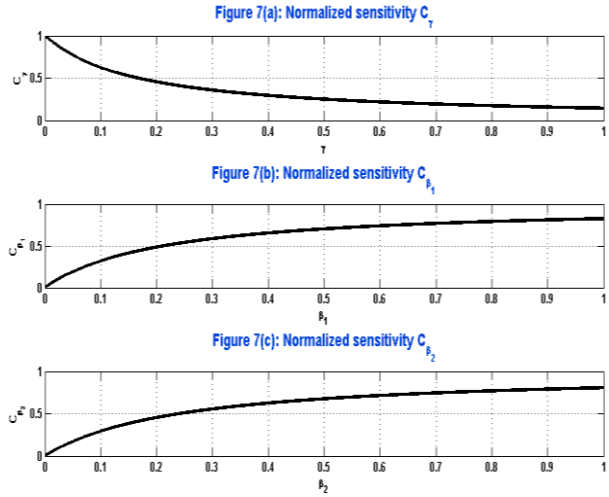

Figure 7. Local sensitivity analysis: Normalized sensitivity indices

Figure 7(a) shows that the normalized sensitivity with respect to γ decreases monotonically, indicating that larger γ values consistently diminish its contribution to variations in $\mathcal{R}_0$. Figure 7(b) indicates that the sensitivity to β_1 increases nonlinearly, implying that direct transmission becomes progressively more influential in shaping $\mathcal{R}_0$ as β_1 increases. Meanwhile, Figure 7(c) exhibits a more gradual increase in sensitivity to β_2, with a gentler slope than that of β_1, suggesting that vector-mediated transmission contributes positively to $\mathcal{R}_0$ but with a comparatively moderate effect.

The normalized sensitivity indices for γ, β_1, and β_2, along with their corresponding interpretations, are summarized in Table 3.

Table 3. The results of the sensitivity index calculation

Parameter	Sensitivity Index	Interpretation
$C_{\beta_1} = 0.65$	The highest value	A 1% increase in β_1 results in a 0.65% increase $\mathcal{R}_0$
$C_{\beta_2} = 0.35$	Moderate	A 1% increase in β_2 results in a 0.35% increase $\mathcal{R}_0$
$C_\gamma = 0.06$	Low	A 1% increase in γ results in a 0.06% increase $\mathcal{R}_0$

This study analyzes local sensitivity by focusing on the parameters γ, β_1 and β_2, yielding the following results. The sensitivity analysis presented in Table 3 identifies β_1 and β_2 as the most influential parameters. Consequently, control strategies should prioritize reducing these parameters by enhancing biosecurity measures and minimizing contact between pigs and vector ticks.

4. DISCUSSIONS

This study is the first to examine ASF transmission in East Nusa Tenggara and, more broadly, the first in Indonesia to analyze its dynamics using a mathematical modeling approach. The results indicate that $\mathcal{R}_{01}$ = 2.35 in the absence of tick vector involvement, whereas with vector involvement,

$\mathcal{R}_0$ = 3.5. Since the value of $\mathcal{R}_0$ remains well above unity, this indicates that ASF transmission in East Nusa Tenggara continues, and the disease persists within the pig population. This result is consistent with the findings of previous studies [8-27]. Effective control of ASF requires the implementation of strategic measures. These measures include improved biosecurity, disease surveillance, the establishment of ASF-free compartments, ongoing vaccine research and evaluation, and the strengthening of veterinary services. We applied biosecurity strategies and controlled contact between susceptible pigs and ASF-infected tick vectors to assess the reduction in the exposed compartment and the basic reproduction number, with the following results. At a biosecurity and vector control coverage of $p = q = 50\%$, the transmission effectiveness in the exposed compartment decreased by 17.48% with a reproduction number ($\mathcal{R}_0$) of 1.775. Increasing coverage to $p = q = 65\%$, reduced it to 22.73% ($\mathcal{R}_0$ = 1.2425), while at $p = q = 72\%$, the reduction reached 25.18% ($\mathcal{R}_0 = 0.994$), indicating a state near the control threshold. At higher coverage $p = q = 85\%$, a 29.72% reduction with $\mathcal{R}_0 = 0.5325$ confirmed that the epidemic can be effectively controlled. Based on mathematical modeling analysis, this study demonstrates that an integrated strategy of biosecurity and vector control is effective in reducing the spread of ASF in East Nusa Tenggara, Indonesia. Field evidence also indicates that the local practice of installing nets in pig pens is effective in controlling ASF. These findings are consistent with those of Boklund et al. [28] and Olesen et al. [29], who demonstrated that installing nets in pig pens is effective in controlling tick vectors and reducing the risk of ASF transmission.

5. CONCLUSIONS

The results show that ASF in East Nusa Tenggara is still spreading at a high level, with $\mathcal{R}_{01} = 2.35$ and $\mathcal{R}_0 = 3.5$, indicating continued infection in the pig population. Numerical simulation indicates that a combination of enhanced biosecurity and vector control is effective in suppressing transmission. These findings emphasize the need for strengthened biosecurity policies, community-based vector control, and ongoing surveillance. This model has limitations due to its assumption of homogeneous mixing and simplification of host-vector interactions, necessitating field validation and the development of further stochastic models.

ACKNOWLEDGMENT

Our research funding comes from the Mathematics Study Program, Faculty of Science and Engineering, Nusa Cendana University (Grant No.: 247/UN15.22/PL/2025) dated on 26th March 2025.

REFERENCES

[1] Ciputra, L.A., Rahman, A.S., Nurfadhillah, B., Masyita, et al. (2023). African swine fever and its socio-economic impacts in Indonesia. Media Kedokteran Hewan, 34(3) 171-182. https://doi.org/10.20473/mkh.v34i3.2023.171-182

[2] Kouidere, A., Balatif, O., Rachik, M. (2021). Analysis and optimal control of a mathematical modeling of the spread of African swine fever virus with a case study of South Korea and cost-effectiveness. Chaos, Solitons & Fractals, 146: 110867. https://doi.org/10.1016/j.chaos.2021.110867

[3] Sukoco, H., Salmin, S., Wahyuni, S., Utami, S., et al. (2024). African swine fever (ASF): Etiology, pathogenesis, clinical symptoms, transmission, prevention and control in pigs. Jurnal Pertanian Agros, 26(1): 4412-4426.

[4] HA, A., Tulle, R.D. (2023). Seroprevalence rate and factors causing African swine fever outbreak in Kupang City and Regency of East Nusa Tenggara Province, Indonesia. EAS Journal of Veterinary Medical Science, 5(2): 12-19. https://doi.org/10.36349/easjvms.2023.v05i02.001

[5] Zhang, T., Qin, X., Dong, S., Wu, Y., et al. (2025). African swine fever virus MGF 360-2L disrupts host antiviral immunity based on transcriptomic analysis. Vaccines, 13(9): 918. https://doi.org/10.3390/vaccines13090918

[6] Klein, L., Gerdes, U., Blome, S., Campe, A., Große Beilage, E. (2024). Biosecurity measures for the prevention of African swine fever on German pig farms: Comparison of farmers' own appraisals and external veterinary experts' evaluations. Porcine Health Management, 10(1): 14. https://doi.org/10.1186/s40813-024-00365-x

[7] Chuchard, P., Prathumwan, D., Trachoo, K., Maiaugree, W., Chaiya, I. (2022). The SLI-SC mathematical model of African swine fever transmission among swine farms: The effect of contaminated human vector. Axioms, 11(7): 329. https://doi.org/10.3390/axioms11070329

[8] Ayihou, S.Y., Doumatè, T.J., Hameni Nkwayep, C., Bowong Tsakou, S., Glèlè Kakai, R. (2024). Mathematical modeling and transmission dynamics analysis of the African swine fever virus in Benin. Mathematics, 12(11): 1749. https://doi.org/10.3390/math12111749

[9] Kouidere, A., Balatif, O., Rachik, M. (2023). Fractional optimal control problem for a mathematical modeling of African swine fever virus transmission. Moroccan Journal of Pure and Applied Analysis, 9(1): 97-110. https://doi.org/10.2478/mjpaa-2023-0007

[10] Bulu, P.M., Paga, A., Lasakar, A.S., Wera, E. (2023). Pig farm management and its contribution to the African Swine Fever incidences in Kupang, Indonesia. Jurnal Medik Veteriner, 6(2): 155-161. https://doi.org/10.20473/jmv.vol6.iss2.2023.155-161

[11] Pandarangga, P., Ticoalu, A.E., Gelolodo, M.A.A., Toha, L.R. (2023). Development of highly sensitive conventional PCR for African swine fever virus diagnosis in East Nusa Tenggara (NTT) Province. Jurnal Kajian Veteriner, 11(2): 218-224. https://doi.org/10.35508/jkv.v11i2.13118

[12] Bani-Yaghoub, M., Gautam, R., Shuai, Z., Van Den Driessche, P., Ivanek, R. (2012). Reproduction numbers for infections with free-living pathogens growing in the environment. Journal of Biological Dynamics, 6(2): 923-940. https://doi.org/10.1080/17513758.2012.693206

[13] Ndii, M.Z., Anggriani, N., Messakh, J.J., Djahi, B.S. (2021). Estimating the reproduction number and designing the integrated strategies against dengue.

Results in Physics, 27: 104473. https://doi.org/10.1016/j.rinp.2021.104473
[14] Achaiah, N.C., Subbarajasetty, S.B., Shetty, R.M. (2020). R0 and Re of COVID-19: Can we predict when the pandemic outbreak will be contained? Indian Journal of Critical Care Medicine, 24(11): 1125. https://doi.org/10.5005/jp-journals-10071-23649
[15] Dayap, J.A., Rabajante, J.F. (2025). Mathematical model of dengue transmission dynamics with adaptive human behavior. Communication in Biomathematical Sciences, 8(1): 93-109. https://doi.org/10.5614/cbms.2025.8.1.7
[16] Sasongko, P.S., Brilliant, M., Triyana, E. (2022). Mathematical modeling and stability analysis of the COVID-19 spread by considering quarantine and hospitalize. Mathematical Modelling of Engineering Problems, 9(6): 1545-1556. https://doi.org/10.18280/mmep.090614
[17] Jafaruddin, Indratno, S.W., Nuraini, N., Supriatna, A.K., Soewono, E. (2015). Estimation of the basic reproductive ratio for dengue fever at the take-off period of dengue infection. Computational and Mathematical Methods in Medicine, 2015(1): 206131. https://doi.org/10.1155/2015/206131
[18] Guan, R., Wu, J., Wang, Y., Cai, Q., Li, X. (2023). Comparative analysis of productive performance and fattening efficiency of commercial pigs in China for two consecutive years. Scientific Reports, 13(1): 8154. https://doi.org/10.1038/s41598-023-35430-y
[19] Das, S., Deka, P., Deka, P., Kalita, K., Ansari, T., Hazarika, R., Barman, N.N. (2021). African swine fever: Etiology, epidemiology, control strategies and progress toward vaccine development: A comprehensive review. Journal of Entomology and Zoology Studies, 9(1): 919-929.
[20] Sendow, I., Ratnawati, A., Dharmayanti, N.L.P.I., Saepulloh, M. (2020). African swine fever: Penyakit emerging yang mengancam peternakan babi di dunia. Indonesian Bulletin of Animal and Veterinary Sciences, 30(1): 15.
[21] Lv, T.B., Xie, X.F., Song, N., Zhang, S.L., et al. (2022). Expounding the role of tick in Africa swine fever virus transmission and seeking effective prevention measures: A review. Frontiers in Immunology, 13: 1-12. https://doi.org/10.3389/fimmu.2022.1093599
[22] Barongo, M.B., Ståhl, K., Bett, B., Bishop, R.P., et al. (2015). Estimating the basic reproductive number (R0) for African swine fever virus (ASFV) transmission between pig herds in Uganda. PloS One, 10(5): e0125842. https://doi.org/10.1371/journal.pone.0125842
[23] Marcon, A., Linden, A., Satran, P., Gervasi, V., Licoppe, A., Guberti, V. (2020). R0 estimation for the African swine fever epidemics in wild boar of Czech Republic and Belgium. Veterinary Sciences, 7(1): 2. https://doi.org/10.3390/vetsci7010002
[24] Çakan, S. (2022). Local asymptotic stability and sensitivity analysis of a new mathematical epidemic model without immunity. Mathematical Sciences and Applications E-Notes, 10(1): 50-62. https://doi.org/10.36753/mathenot.935016
[25] Hurint, R.U., Ndii, M.Z., Lobo, M. (2017). Analisis sensitivitas model epidemi SEIR sensitivity analysis of seir epidemic model. Online Journal of Natural Science, 6(1): 22-28. https://doi.org/10.22487/25411969.2017.v6.i1.8076
[26] Mohandoss, A., Chandrasekar, G., Jan, R. (2023). Modelling and analysis of vaccination effects on hand, foot, and mouth disease transmission dynamics. Mathematical Modelling of Engineering Problems, 10(6): 1937-1949. https://doi.org/10.18280/mmep.100603
[27] Matsumoto, N., Ward, M.P., Halasa, T., Schemann, K., et al. (2024). Novel estimation of African swine fever transmission parameters within smallholder villages in Lao PDR. Tropical Animal Health and Production, 56(5): 166. https://doi.org/10.1007/s11250-024-04012-z
[28] Boklund, A.E., Ståhl, K., Miranda Chueca, M.Á., et al. (2024). Risk and protective factors for ASF in domestic pigs and wild boar in the EU, and mitigation measures for managing the disease in wild boar. EFSA Journal, 22(12): e9095. https://doi.org/10.2903/j.efsa.2024.9095
[29] Olesen, A.S., Stelder, J.J., Tjørnehøj, K., Johnston, C.M., et al. (2023). Detection of African swine fever virus and blood meals of porcine origin in hematophagous insects collected adjacent to a high-biosecurity pig farm in Lithuani; a smoking gun? Viruses, 15(6): 1255. https://doi.org/10.3390/v15061255